ISSN 1063-7761, Journal of Experimental and Theoretical Physics, 2011, Vol. 113, No. 3, pp. 483–489. © Pleiades Publishing, Inc., 2011.
Original Russian Text © A.I. Pankrats, G.A. Petrakovskii, V.I. Tugarinov, A.V. Kartashev, V.L. Temerov, 2011, published in Zhurnal Eksperimental'noi i Teoreticheskoi Fiziki, 2011, Vol. 140, No. 3, pp. 553–560.

ORDER, DISORDER, AND PHASE TRANSITION IN CONDENSED SYSTEM

Magnetic-Resonance and Thermophysical Studies of the Magnetic Phase Diagram for a $GdFe_{2.1}Ga_{0.9}(BO_3)_4$ Single Crystal

A. I. Pankrats, G. A. Petrakovskii, V. I. Tugarinov*, A. V. Kartashev, and V. L. Temerov

Kirensky Institute of Physics, Russian Academy of Science, Siberian Branch, Krasnoyarsk, 660036 Russia

**e-mail: vit@iph.krasn.ru*

Received December 30, 2010

Abstract—The antiferromagnetic resonance, heat capacity, magnetic properties, and magnetic phase diagram of a $GdFe_3(BO_3)_4$ crystal in which some of the iron ions were substituted by diamagnetic gallium ions have been investigated. It has been found that the Neél temperature upon diamagnetic substitution decreased to 17 K compared to 38 K in the unsubstituted crystal. The effective exchange and anisotropy fields for $GdFe_{2.1}Ga_{0.9}(BO_3)_4$ have been estimated from the field dependences of magnetization and resonance measurements. The magnetic phase diagram of the crystal has been constructed from magnetic and resonance measurements. In $GdFe_{2.1}Ga_{0.9}(BO_3)_4$, there is no spontaneous reorientation and, in the absence of a magnetic field, the crystal remains an easy-axis one in the entire domain of magnetic ordering. The critical field of the reorientation transition to an induced easy-plane state in a magnetic field along the trigonal axis has been found to increase compared to that in the unsubstituted crystal.

DOI: 10.1134/S1063776111070089

1. INTRODUCTION

Borate compounds with the general formula $RA_3(BO_3)_4$ (R^{3+} is a rare-earth ion or Y^{3+} and A = Al, Ga, Sc, Cr, Fe) have attracted attention as a medium for nonlinear optics and laser technology [1–3]. They are crystallized in trigonal syngony and have the structure of the huntite mineral with a high-temperature space group $R32$ that transforms into $P3_121$ for crystals with a small ionic radius R^{3+} as the temperature decreases. In crystals with A = Fe and R = Pr, Nd, Sm, Eu, Gd, Tb, Dy, Ho, and Er, the properties of multiferroics were found [4–7]. The magnetoelectric effect is possible only for a certain magnetic structure that, in the case under consideration, is determined by the coexistence of two magnetic subsystems of iron ions and rare-earth ions coupled by the exchange interaction. This stimulates interest in investigating the dependence of the magnetic properties of rare-earth ferroborates on the R^{3+} ion.

Antiferromagnetic-resonance (AFMR) studies [8] and neutron studies of the magnetic structure [9] in $YFe_3(BO_3)_4$ show that the iron subsystem is an easy-plane antiferromagnet with the Neél temperature $T_N = 38$ K. In the rare-earth subsystem, the exchange interaction is weak, but magnetic order in both subsystems sets in simultaneously due to the interaction of rare-earth ions with Fe^{3+} ions [8, 10]. The anisotropy energy of the rare-earth subsystem can have the same sign as the iron one, but it can be an easy-axis one. This makes it possible to realize a number of magnetic crystal structures depending on the R^{3+} ion. Ferroborates with R = Cd, Ho are particularly interesting in this respect. In gadolinium ferroborate $GdFe_3(BO_3)_4$, the contributions from the rare-earth and iron subsystems are opposite in sign and close in absolute value [8, 11]. Therefore, the magnetic structure of this crystal is very sensitive to the action of such factors as the temperature, the magnetic field, and the substitution by ions of a different type in both subsystems, which change the ratio of the contributions to the total anisotropy. The difference between their temperature dependences (AFMR data [8]) leads to a spontaneous spin-reorientation transition in $GdFe_3(BO_3)_4$ with $T_{SR} = 10$ K. The magnetic phase diagrams of this crystal for magnetic fields oriented along the crystal axis and in the basal plane were constructed from AFMR data [11], magnetic [12], magnetostriction and magnetoelectric measurements [4]. In $HoFe_3(BO_3)_4$, the spontaneous reorientation transition occurs at $T_{SR} =$ 4.7 K [9]; the magnetic phase diagrams are given in [13].

The magnetic properties of the gadolinium subsystem in $GdFe_3(BO_3)_4$ partially or completely substituted by the diamagnetic Y^{3+} ion were studied in [8]. Studying the influence of the substitution of the iron subsystem by a diamagnetic impurity is of considerable interest, because, in this case, not only the contribution from this subsystem to the magnetic anisotropy of the crystal but also the exchange interaction changes. The latter is fundamentally important for the establishment of magnetic order in the crystal. The static magnetic properties of gallium-substituted gadolinium ferroborate $GdFe_{0.9}Ga_{2.1}(BO_3)_4$ were investigated in [14]. An anomaly whose nature was not explained was detected in the temperature depen-

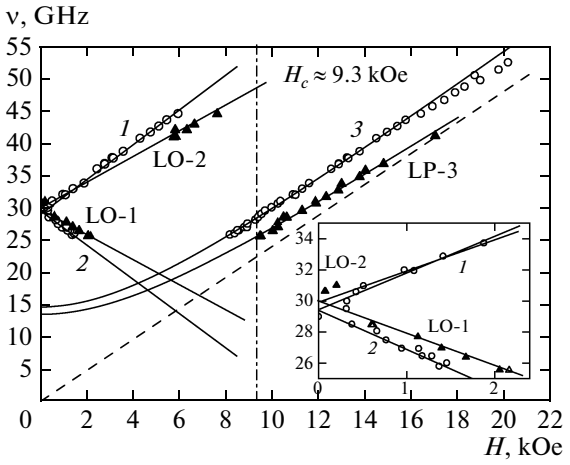

Fig. 1. Frequency–field dependences of the AFMR at $T = 4.2$ K for **H** ∥ **c**: curves *1*, *2*, *3* are the branches for $GdFe_3(BO_3)_4$ [11]; LO-1, LO-2, LP-3 are the branches for $GdFe_{2.1}Ga_{0.9}(BO_3)_4$. The dashed line is the paramagnetic resonance branch; the dash–dotted line is the critical field in $GdFe_{2.1}Ga_{0.9}(BO_3)_4$. The inset shows branches *1*, *2* and LO-1, LO-2 in the region of initial spectral splitting.

dence of magnetization near $T = 15$ K. Here, we investigate the magnetic resonance and heat capacity of the compound $GdFe_{2.1}Ga_{0.9}(BO_3)_4$. An anomaly of the heat capacity caused by the transition to the magnetically ordered state of a diamagnetically diluted iron subsystem was detected near 17 K. We established that the crystal remains an easy-axis one in the entire domain of magnetic order. In a magnetic field applied along the trigonal axis of the crystal, we detected the transition to an induced easy-plane state and constructed the phase diagram for this field orientation. We estimated the effective magnetic anisotropy and exchange interaction fields for a diluted iron subsystem.

2. EXPERIMENTAL RESULTS

The $GdFe_{2.1}Ga_{0.9}(BO_3)_4$ single crystals were grown using the technology described in [15]. The AFMR spectra were measured on well-faceted samples up to $3 \times 3 \times 3$ mm^3 in size. A face in the form of an equilateral triangle coincident with the crystal basal plane was used to orient the crystals. The resonance properties were studied in the frequency range 25–80 GHz in the range of temperatures 4.2–60 K in magnetic fields **H** ∥ **c** and **H** ⊥ **c** on a magnetic resonance spectrometer with a pulsed magnetic field [16]. The heat capacity was measured on a $2 \times 2 \times 1$ mm^3 single-crystal sample on PPMS-8.

In $GdFe_{2.1}Ga_{0.9}(BO_3)_4$, the same oscillation branches (Fig. 1) as those in unsubstituted $GdFe_3(BO_3)_4$ [11] are observed at a temperature of 4.2 K for a magnetic field oriented along the trigonal axis. The frequency–field dependences of the AFMR spectra in $GdFe_3(BO_3)_4$ are also presented in Fig. 1 for comparison. In the range of weak fields, the two oscillation branches LO-1 and LO-2 with a linear dependence of the frequencies on magnetic field are the oscillations of an easy-axis antiferromagnet. When some critical field H_c indicated in Fig. 1 by the dash–dotted lines is reached, the resonance branches LO-1 and LO-2 vanish and only one oscillation branch with a gap that changed insignificantly compared to the gap in the unsubstituted crystal is observed in fields $H > H_c$ instead of them. This oscillation branch cannot be considered as the spin-flop mode of an easy-axis antiferromagnet, because the frequency of this mode is nonzero in the transition field and the branch itself lies not below the linear frequency–field dependence for the paramagnetic resonance (the dashed line in the figure), as should be for the spin-flop resonance, but above it. This behavior of the resonance is typical of the range of fields above the critical ones in both pure and diamagnetically diluted gadolinium ferroborates. It gives empirical grounds for identifying this resonance mode as the oscillations of an easy-plane antiferromagnet with some new value of the effective anisotropy field.

Thus, the phase transition at $H = H_c$ may be considered as the spin-reorientation transition from an easy-axis state to a field-induced easy-plane one.

The critical field of the spin-reorientation "easy axis–easy plane" transition as a result of dilution by gallium at $T = 4.2$ K increased from $H_c = 6$ kOe to $H_c = 9.3$ kOe. As we see from Fig. 2, a new oscillation branch, LP-3, appears above this field (Fig. 1). This branch is close to the oscillation branch in the induced easy-plane state in $GdFe_3(BO_3)_4$ with the virtually unchanged initial splitting.

Figure 2 shows the change of the AFMR spectra in $GdFe_{2.1}Ga_{0.9}(BO_3)_4$ with temperature in the range 4.2–12 K at a frequency of 25.56 GHz in a magnetic field **H** ∥ **c**. Two resonance absorption lines are observed at a temperature of 4.2 K. The designations near the lines correspond to those on the frequency–field dependence in Fig. 1. The resonance field of the line LO-1 gradually decreases with rising temperature to zero at $T \approx 5$ K (Fig. 3). The resonance field of the line LO-2 that appears above $T = 5$ K gradually increases almost to the resonance field of the paramagnetic state (Fig. 3). The line LP-3 at low temperatures is outlined incompletely, because the corresponding absorption is cut off in the critical field H_c. For this reason, it is difficult to determine the resonance field at these temperatures. This feature in the form of a line break for the gallium-substituted crystal is observed up to a temperature of 12 K owing to the large width of the resonance absorption line ($\Delta H \approx 1.5$ kOe at $T = 4.2$ K) and the very weak temperature dependence of the transition field H_c. It can be concluded from the temperature dependence of the resonance fields for the lines LO-1, LO-2, and LP-3 that

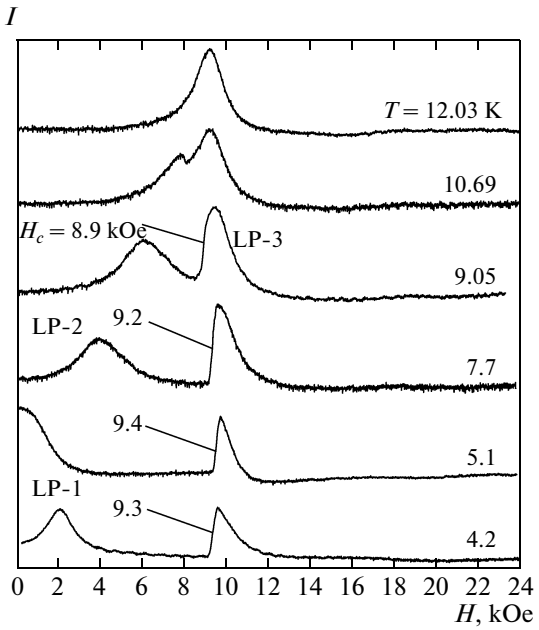

Fig. 2. Temperature evolution of the resonance spectrum in $GdFe_{2.1}Ga_{0.9}(BO_3)_4$ at $\nu = 25.56$ GHz, $\mathbf{H} \parallel \mathbf{c}$.

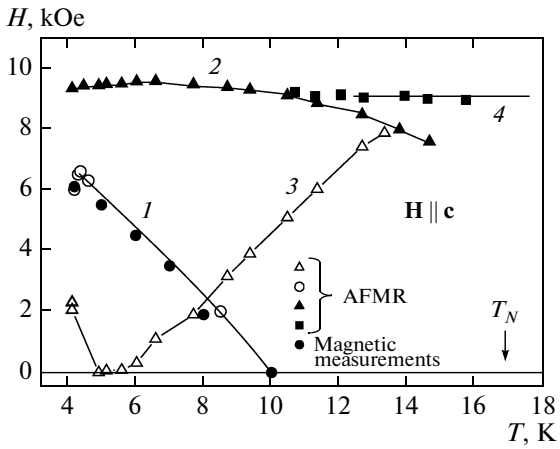

Fig. 3. Temperature dependences of the critical fields for $\mathbf{H} \parallel \mathbf{c}$: curves *1* and *2* are for $GdFe_3(BO_3)_4$ and $GdFe_{2.1}Ga_{0.9}(BO_3)_4$, respectively. The temperature dependences of the resonance fields in $GdFe_{2.1}Ga_{0.9}(BO_3)_4$: curves *3* and *4* are the branches LO-1 and LO-2; curve *4* is the branch LP-3. The data were obtained at $\nu = 25.56$ GHz.

the gap decreases monotonically with rising temperature for both easy-axis and easy-plane states.

Having analyzed the magnetic resonance spectra, we constructed the temperature dependences of the resonance field for the branches LO-1, LO-2, and LP-3 and the critical field of the "easy axis–easy plane" transition in Ga-substituted $GdFe_3(BO_3)_4$ for $\mathbf{H} \parallel \mathbf{c}$ (Fig. 3). The data for unsubstituted $GdFe_3(BO_3)_4$ taken from [11] are also shown here for comparison. We see that the critical field of the transition to the induced easy-plane state for this magnetic field direction increased compared to unsubstituted gadolinium ferroborate. In addition, since the phase boundary in $GdFe_{2.1}Ga_{0.9}(BO_3)_4$ has a very weak temperature dependence compared to the unsubstituted crystal, no tendency toward the spontaneous spin-reorientation transition to the easy-plane state was found in this crystal. The temperature dependence of the resonance field in the easy-axis state (curve *3*) measured at a frequency of 25.56 GHz is similar in form to the dependence for unsubstituted gadolinium ferroborate [11]. The frequency dependence of the resonance field in the field-induced easy-plane state for $\mathbf{H} \parallel \mathbf{c}$ near the transition temperature is similar to the dependence for the electron paramagnetic resonance (EPR). Therefore, the temperature dependence of the resonance parameters for this oscillation branch (line *4* in Fig. 3) exhibits no features, except the line broadening during the transition to the paramagnetic state.

The temperature dependence of the resonance field in $GdFe_{2.1}Ga_{0.9}(BO_3)_4$ for a magnetic field $\mathbf{H} \perp \mathbf{c}$ is shown in Fig. 4. For comparison, the same figure presents the temperature dependence of the resonance field in $GdFe_3(BO_3)_4$ taken at a close frequency [11]. We see that a jump in resonance field caused by the transition to the induced easy-plane state is observed in $GdFe_3(BO_3)_4$. For $GdFe_{2.1}Ga_{0.9}(BO_3)_4$, the situation is different: no jump is observed, the resonance field gradually reaches a plateau at $T \approx 16$ K and does not change as the temperature rises further.

Figure 5 shows the temperature dependences of the heat capacity of $GdFe_{2.1}Ga_{0.9}(BO_3)_4$ for various magnetic fields. We see from the figure that the anomaly of the heat capacity at a temperature of about 17 K has the typical form of a λ peak and is virtually independent of the magnitude and direction of the magnetic field.

3. DISCUSSION OF RESULTS

Since only one λ peak is present in the range of temperatures up to 300 K, it can be said with confidence that 17 K is the Neél temperature for the compound under consideration. The temperature dependence of the heat capacity for pure $GdFe_3(BO_3)_4$ is given in [17]; comparison shows that the Neél temperature upon dilution of the iron subsystem decreased from 38 K more than twofold. This conclusion is confirmed by magnetization measurements, in which an anomaly is observed at a temperature close to 15 K and no anomalies have been detected above this temperature [14]. The temperature dependences of the resonance fields also exhibit a plateau near 16 K corresponding to the EPR line. The decrease in Neél temperature is quite natural; it is attributable to a reduction in the exchange field for the iron subsystem upon diamagnetic dilution. Such a situation was observed upon diamagnetic dilution in other crystals

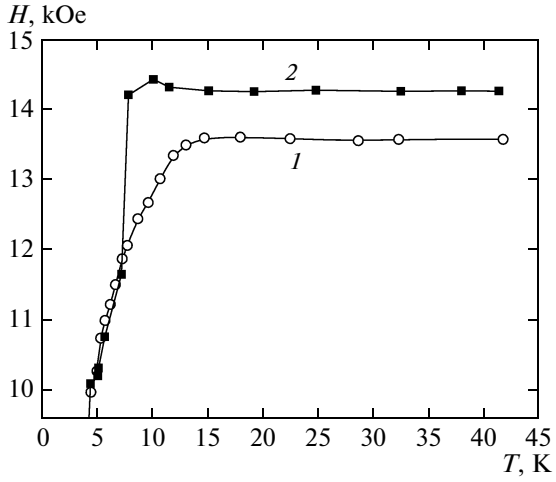

Fig. 4. Temperature dependences of the resonance fields in $GdFe_{2.1}Ga_{0.9}(BO_3)_4$ (*1*) and $GdFe_3(BO_3)_4$ [11] (*2*), respectively, at $\nu = 37.63$ and 38.63 GHz for $\mathbf{H} \perp \mathbf{c}$.

(e.g., in $Rb_2Mn_xCd_{1-x}Cl_4$, the Neél temperature upon dilution to $x = 0.7$ decreased from 56 to 10.7 K [18]).

The magnetic phase diagram (Fig. 6) in $GdFe_{2.1}Ga_{0.9}(BO_3)_4$ for $\mathbf{H} \parallel \mathbf{c}$ constructed from heat-capacity, resonance, and magnetic measurements contains three states: the paramagnetic one above $T_N = 17$ K and the easy-axis and induced easy-plane ones, respectively, below and above the phase boundary. Thus, dilution not only reduced the Neél temperature but also changed significantly the phase diagram for $GdFe_3(BO_3)_4$. The main distinction is the absence of a spontaneous "easy axis–easy plane" transition, while the spontaneous transition is observed at $T = 10$ K in pure gadolinium ferroborate (Fig. 3). The phase boundary between the induced easy-plane and easy-axis states lies higher (at $T = 4.2$ K, $H_c = 10$ kOe in $GdFe_{2.1}Ga_{0.9}(BO_3)_4$ and $H_c = 6$ kOe in $GdFe_3(BO_3)_4$) and, in contrast to $GdFe_3(BO_3)_4$, has a very weak temperature dependence. In a diluted crystal for a magnetic field $\mathbf{H} \perp \mathbf{c}$, no induced easy-plane state was detected in fields up to 60 kOe. All these facts are indicative of a great change in the internal effective exchange and anisotropy fields, which can be estimated by analyzing the magnetic-resonance and magnetization data.

It should be noted that as yet there is no consistent model for the description of field-induced spin-reorientation transitions in gadolinium ferroborate, in both pure and diamagnetically diluted ones. Therefore, the identification of states in the phase diagram presented here is based on an empirical approach. As has been noted above, the total magnetic anisotropy of the $GdFe_3(BO_3)_4$ crystal is determined by the competition between the contributions from the subsystems of Fe^{3+} and Gd^{3+} ions that are close in absolute value and opposite in sign. In this case, even a slight change in one of the contributions leads to a significant change of their balance. Therefore, the magnetic structure of gadolinium ferroborate is very sensitive to both magnetic field and diamagnetic substitution in one of the subsystems. A similar situation is observed in holmium ferroborate, in which the competition between the contributions close in magnitude also leads to the spontaneous transition between the easy-axis and easy-plane states at $T_{SR} = 4.7$ K and the dependence of the transition temperature on the magnetic field applied along the crystal axis and in the basal plane [9, 13]. The authors of [19] managed to quantitatively describe both spontaneous and field-induced spin-reorientation transitions between the easy-axis and easy-plane states in $HoFe_3(BO_3)_4$ in terms of the crystal-field model for Ho^{3+} and the molecular-field

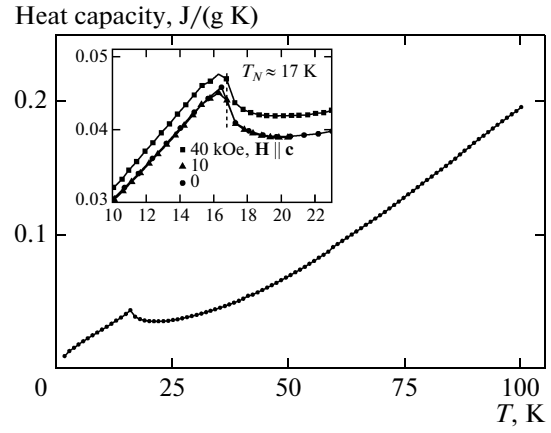

Fig. 5. Temperature dependence of the heat capacity in $GdFe_{2.1}Ga_{0.9}(BO_3)_4$. The inset shows the temperature dependences of the heat capacity in the transition region for various directions and magnitudes of the magnetic field.

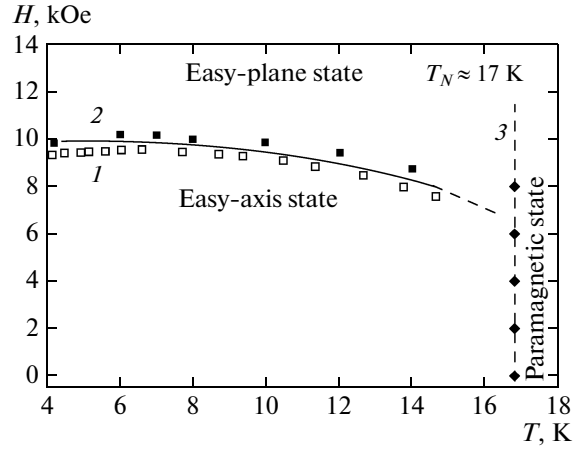

Fig. 6. Magnetic phase diagram in $GdFe_{2.1}Ga_{0.9}(BO_3)_4$ constructed from AFMR data (*1*), static magnetic measurements (*2*), and heat capacity (*3*).

approximation. The calculations performed in the above paper show that the magnetic-anisotropy contribution from the holmium subsystem depends on the applied magnetic field, which causes the sign of the total crystal anisotropy in the critical field to change. A similar spin-reorientation transition mechanism probably also works in gadolinium ferroborate.

The magnetic resonance in gadolinium ferroborate in the region of magnetic order is determined by the coupled oscillations of the magnetic moments of Fe^{3+} ions and the magnetic moments of Gd^{3+} ions polarized by the exchange interaction with the ordered iron subsystem. However, the eigenfrequencies of the iron and gadolinium subsystems are spaced widely apart (according to the data of [20], the eigenfrequencies of the iron and gadolinium subsystems lie in the range 420–510 GHz). Therefore, the resonance response observed in our case is determined predominantly by the iron subsystem and it is quite admissible to use the expressions for a classical two-sublattice antiferromagnet [21] to describe the oscillation branches, as was done in [11]. In this case, the role of the rare-earth subsystem is reduced to the fact that its contribution changes the total effective magnetic anisotropy field. The branches LO-1 and LO-2 of the frequency–field dependence (Fig. 1) in a magnetic field $\mathbf{H} \parallel \mathbf{c}$ observed in fields below the critical one ($H < H_c$) are well described by the expressions for an easy-axis antiferromagnet:

$$\frac{\nu_{1,2}}{\gamma_{\parallel}} = \sqrt{(2H_E + H_A)H_A} \pm H_0\left(1 - \frac{\chi_{\parallel}}{2\chi_{\perp}}\right). \quad (1)$$

As regards the oscillation branch LP-3 in fields above the critical ones, in accordance with the above empirical grounds, these oscillations were approximated by the formula for an easy-plane antiferromagnet:

$$\left(\frac{\nu_3}{\gamma_{\parallel}}\right)^2 = 2H_E\left|H_A'\right| + H_0^2. \quad (2)$$

The following notation is used in the formulas: H_0 is the external magnetic field strength, H_A and H_A' are the effective magnetic anisotropy fields relative to the crystal c axis that have different signs and values in the easy-axis and field-induced easy-plane states, H_E is the exchange field, γ is the gyromagnetic ratio, $\chi_{\parallel}$ and $\chi_{\perp}$ are the magnetic susceptibilities along the principal axis and in the basal plane. In Fig. 1, the solid lines indicate the theoretical dependences (1) for the oscillation branches LO-1 and LO-2 with the following parameters: $\nu_c = 30.0$ GHz and $\gamma_{\parallel}(1 - \chi_{\parallel}/2\chi_{\perp}) = 2.0$ MHz Oe^{-1}. If we use the value of $\gamma_{\parallel} = 2.808$ MHz Oe^{-1} obtained from the EPR at room temperature, then the susceptibility ratio $\chi_{\parallel}/(2\chi_{\perp}) = 0.29$ (this is close to the experimental value of 0.3 from the data of [14]). This value is considerably higher than that in unsubstituted $GdFe_3(BO_3)_4$, where this ratio is 0.083. Both the large difference in $\chi_{\parallel}/(2\chi_{\perp})$ and the decrease in Neél temperature are related to the reduction in exchange field upon diamagnetic dilution.

In the easy-axis state, the initial spectral splitting ν_c in $GdFe_{2.1}Ga_{0.9}(BO_3)_4$ at a temperature of 4.2 K increased only slightly, by about 1 GHz, compared to gadolinium ferroborate. This can be qualitatively explained as follows. In the easy-axis state, the contribution from the gadolinium subsystem to the total crystal anisotropy does not exceed the contribution from the iron subsystem in absolute value, while partial substitution of iron ions by diamagnetic Ga^{3+} ions additionally reduces this contribution, causing the total anisotropy field to increase. On the other hand, diamagnetic substitution of the iron subsystem reduces the exchange field. As a result of the competition between these two factors, the energy gap upon dilution remains virtually unchanged, but the temperature dependence of the gap changed. Let us compare the temperature dependences of the resonance field in Fig. 4 in pure and Ga-substituted $GdFe_3(BO_3)_4$ for the field orientation $\mathbf{H} \perp \mathbf{c}$. For unsubstituted $GdFe_3(BO_3)_4$, the temperature dependence of the resonance field exhibits a jump near 8 K corresponding to the transition from the easy-axis state to the easy-plane one [11]. Thereafter, the resonance field does not change, because the frequency–field dependences for this AFMR branch and the EPR coincide. In $GdFe_{2.1}Ga_{0.9}(BO_3)_4$, the resonance field gradually increases to a value corresponding to the EPR in the temperature range 4.2–16 K. Thus, the energy gap gradually decreases with rising temperature, reaching zero at the Neél temperature. The absence of a jump in resonance field suggests that no transition to the induced easy-plane state is observed in the $GdFe_{2.1}Ga_{0.9}(BO_3)_4$ crystal for a magnetic field $\mathbf{H} \perp \mathbf{c}$, at least in magnetic fields up to 60 kOe. The weak temperature dependence of the critical field for the transition to the induced state for $\mathbf{H} \parallel \mathbf{c}$ up to the Neél temperature suggests the absence of a spontaneous "easy axis–easy plane" transition, which is confirmed by magnetic measurements [14].

Let us estimate the anisotropy and exchange fields in $GdFe_{2.1}Ga_{0.9}(BO_3)_4$ at a temperature of 4.2 K using magnetic-resonance data and static magnetic measurements [14]. The exchange field for the iron subsystem can be obtained from the expression for the magnetic susceptibility $\chi_{\perp}$ of an antiferromagnet

$$\chi_{\perp} = \frac{M_s}{2H_E}. \quad (3)$$

To determine the susceptibility of the diamagnetically diluted iron subsystem in $GdFe_{2.1}Ga_{0.9}(BO_3)_4$, we used static magnetic measurements in the $GdFe_3(BO_3)_4$ [14] and $YFe_3(BO_3)_4$ [6] crystals. The total magnetization of gadolinium ferroborate (curve *2* in Fig. 7) is the sum of the magnetizations of the iron and gadolinium subsystems, $\mu_{FeGd} = \mu_{Gd} + \mu_{Fe}$.

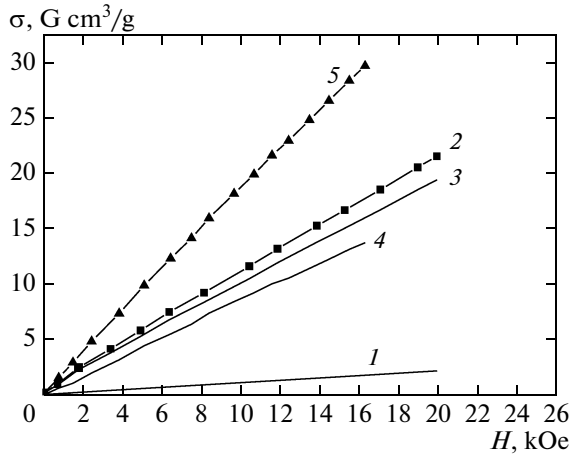

Fig. 7. Field dependence of the magnetization in $GdFe_3(BO_3)_4$ (*2*), $YFe_3(BO_3)_4$ (*1*), and $GdFe_{2.1}Ga_{0.9}(BO_3)_4$ (*5*) and the calculated contribution from the Fe^{3+} (*4*) and Gd^{3+} (*3*) ions to the total magnetization in $GdFe_{2.1}Ga_{0.9}(BO_3)_4$.

The field dependence of the magnetization of the iron subsystem $\mu_{Fe}(H)$ measured in $YFe_3(BO_3)_4$ [9] has a considerably smaller slope (Fig. 7, curve *1*) than the total magnetization in $GdFe_3(BO_3)_4$, suggesting a significant contribution from the gadolinium subsystem $\mu_{Gd}(H)$. The exchange field calculated from $\mu_{Fe}(H)$ is $H_E^{Fe} \approx 700$ kOe; the magnetic susceptibility for the iron subsystem is $\chi_\perp^{Fe} \approx 0.107 \times 10^{-3}$ cm^3 g^{-1} [6]. Taking this value into account, we obtain the magnetic susceptibility for the gadolinium subsystem $\chi_\perp^{Gd} \approx 0.96 \times 10^{-3}$ cm^3 g^{-1} from the field dependence of the magnetization of $GdFe_3(BO_3)_4$; the field dependence of the gadolinium subsystem is also presented in the figure. Assuming that the contribution from this subsystem $\mu_{Gd}(H)$ in $GdFe_{2.1}Ga_{0.9}(BO_3)_4$ does not change, we obtain the field dependence of the magnetization of the diluted iron subsystem $\mu_{FeGa}(H)$ (curve *4* in Fig. 7) from the total magnetization of this compound (curve *5* in Fig. 7) [13]. The corresponding magnetic susceptibility is $\chi_\perp^{FeGa} \approx 0.85 \times 10^{-3}$ cm^3 g^{-1}, whence the exchange field $H_E^{FeGa} \approx 63$ kOe. When calculating this value, we used the saturation magnetization of the iron subsystem $M_s = 51$ G cm^3 g^{-1} calculated by taking into account the diamagnetic substitution.

We obtain the anisotropy field $H_A^{total} \approx 0.95$ kOe from the expression for the energy gap $\nu_c = 300$ GHz. Assuming that the magnetic anisotropy field of the gadolinium subsystem $H_A^{Gd} = 1.52$ kOe [11] remained unchanged, we obtain the magnetic-anisotropy contribution from the diamagnetically diluted iron subsystem $H_A^{FeGa} = -0.57$ kOe. Compared to $H_A^{Ge} = -1.44$ kOe for unsubstituted $GdFe_3(BO_3)_4$, the anisotropy field H_A^{FeGa} decreases approximately by a factor of 2.5. Note that this method of estimating the exchange and anisotropy fields is approximate, because the magnetizations of the iron and gadolinium subsystems are assumed to be independent here, i.e., the exchange interaction between the subsystems is disregarded. Nevertheless, it is clear that diamagnetic dilution of the iron subsystem reduces its contribution to the magnetic anisotropy of the crystal. In turn, this causes the total anisotropy of the crystal stabilizing the easy-axis state to increase. Probably for this reason, the $GdFe_{2.1}Ga_{0.9}(BO_3)_4$ crystal remains an easy-axis one in the entire domain of existence of magnetic order, while the critical field of the transition to the induced easy-plane state increased almost twofold compared to the unsubstituted crystal.

4. CONCLUSIONS

Our investigation of the AFMR and heat capacity in $GdFe_{2.1}Ga_{0.9}(BO_3)_4$ shows that diamagnetic dilution of the Fe^{3+} ions by gallium ions leads not only to a decrease in the exchange field and a reduction in the Neél temperature but also to a significant change in the magnetic phase diagram. Compared to unsubstituted $GdFe_3(BO_3)_4$, the critical field of the phase transition to the induced easy-plane state for $\mathbf{H} \parallel \mathbf{c}$ increased significantly and has a weak temperature dependence. The phase transition to the induced easy-plane state in a magnetic field lying in the basal plane is not observed, at least in fields up to 60 kOe.

The Neél temperature determined from the heat capacity is 17 K; this value is confirmed by magnetic-resonance data and magnetic measurements. Our estimates show that the exchange field in the iron subsystem decreases as a result of diamagnetic dilution from 700 to 63 kOe, while the contribution from this subsystem to the magnetic anisotropy also decreased from 1.44 to 0.57 kOe. This decrease in the magnetic-anisotropy contribution from the iron subsystem increased the total anisotropy field of the crystal. As a result, there is no spontaneous transition to the easy-plane state in $GdFe_{2.1}Ga_{0.9}(BO_3)_4$ and the crystal remains an easy-axis one in the entire domain of existence of magnetic order.

ACKNOWLEDGMENTS

This work was supported by the Russian Foundation for Basic Research (project no. 10-02-00765a).

REFERENCES

1. D. Jaque, J. Alloys. Compd. **323–324**, 204 (2001).

2. X. Chen, Z. Luo, D. Jaque, J. J. Romero, J. G. Sole, Y. Huang, A. Jiang, and C. Tu, J. Phys.: Condens. Matter **13**, 1171 (2001).
3. A. M. Kalashnikova, V. V. Pavlov, R. V. Pisarev, L. N. Bezmaternykh, M. Bayer, and Th. Rasing, JETP Lett. **80** (5), 293 (2004).
4. A. K. Zvezdin, S. S. Krotov, A. M. Kadomtseva, G. P. Vorob'ev, Yu. F. Popov, A. P. Pyatakov, L. N. Bezmaternykh, and E. A. Popova, JETP Lett. **81** (6), 272 (2005).
5. A. K. Zvezdin, G. P. Vorob'ev, A. M. Kadomtseva, Yu. F. Popov, A. P. Pyatakov, L. N. Bezmaternykh, A. V. Kuvardin, and E. A. Popova, JETP Lett. **83** (11), 509 (2006).
6. A. M. Kadomtseva, Yu. F. Popov, G. P. Vorob'ev, A. A. Mukhin, V. Yu. Ivanov, A. M. Kuz'menko, and L. N. Bezmaternykh, JETP Lett. **87** (1), 39 (2007).
7. A. M. Kadomtseva, Yu. F. Popov, G. P. Vorob'ev, A. P. Pyatakov, S. S. Krotov, K. I. Kamilov, V. Yu. Ivanov, A. A. Mukhin, A. K. Zvezdin, A. M. Kuz'menko, L. N. Bezmaternykh, I. A. Gudim, and V. L. Temerov, Low Temp. Phys. **36** (6), 511 (2010).
8. A. I. Pankrats, G. A. Petrakovskii, L. N. Bezmaternykh, and V. L. Temerov, Phys. Solid State **50** (1), 79 (2008).
9. C. Ritter, A. Vorotynov, A. Pankrats, G. Petrakovskii, V. Temerov, I. Gudim, and R. Szymczak, J. Phys.: Condens. Matter **20**, 365209 (2008).
10. P. Fischer, V. Pomjakushin, D. Sheptyakov, L. Keller, M. Janoschek, B. Roessli, J. Schefer, G. Petrakovskii, L. Bezmaternikh, V. Temerov, and D. Velikanov, J. Phys.: Condens. Matter **18**, 7975 (2006).
11. A. I. Pankrats, G. A. Petrakovskii, L. N. Bezmaternykh, and O. A. Bayukov, JETP **99** (4), 766 (2004).
12. S. A. Kharlamova, S. G. Ovchinnikov, A. D. Balaev, M. F. Thomas, I. S. Lyubutin, and A. G. Gavriliuk, JETP **101** (6), 1098 (2005).
13. A. Pankrats, G. Petrakovskii, A. Kartashev, E. Eremin, and V. Temerov, J. Phys.: Condens. Matter. **21**, 436001 (2009).
14. L. N. Bezmaternykh, S. G. Ovchinnikov, A. D. Balaev, S. A. Kharlamova, V. L. Temerov, and A. D. Vasil'ev, J. Magn. Magn. Mater. **272**, E359 (2004).
15. L. N. Bezmaternykh, V. L. Temerov, I. A. Gudim, and N. A. Stolbovaya, Crystallogr. Rep. **50** (Suppl. 1), 97 (2005).
16. V. I. Tugarinov, I. Ya. Makievskii, and A. I. Pankrats, Instrum. Exp. Tech. **47** (4), 472 (2004).
17. R. Z. Levitin, E. A. Popova, R. M. Chtsherbov, A. N. Vasiliev, M. N. Popova, E. P. Chukalina, S. A. Klimin, P. H. M. van Loosdrecht, D. Fausti, and L. N. Bezmaternykh, JETP Lett. **79** (9), 423 (2004).
18. G. A. Petrakovskii, L. S. Emel'yanova, V. G. Pozdnyakov, and V. K. Korolev, Sov. Phys. Solid State **26** (4), 728 (1984).
19. A. A. Demidov and D. V. Volkov, Phys. Solid State **53** (5), 985 (2011).
20. A. M. Kuzmenko, A. A. Mukhin, V. Yu. Ivanov, A. S. Prokhorov, A. M. Kadomtseva, and L. N. Bezmaternikh, in *Book of Abstracts of the Moscow International Symposium on Magnetism (MISM-2008), Moscow, Russia, June 20–25, 2008* (Moscow, 2008), p. 647.
21. A. G. Gurevich, *Magnetic Resonance in Ferrites and Antiferromagnets* (Nauka, Moscow, 1973) [in Russian].

Translated by V. Astakhov